RADAR OBSERVATIONS OF WAVE FIELD IN LITTORAL ZONE

Stylianos Flampouris, Joerg Seemann, Friedwart Ziemer

GKSS, Max Planck Str. 1, D-21502 Geesthacht, Germany;
stylianos.flampouris@gkss.de; friedwart.ziemer@gkss.de; joerg.seemann@gkss.de

1. INTRODUCTION

The wave breaking and the bottom friction are the two main wave energy dissipation mechanisms. The released energy has significant impact on the nearshore hydrodynamics and sediment dynamics and it has important role in coastal engineering and protection. Nevertheless, the spatial observation of the wave energy dissipation related phenomena in the field is almost impossible with in-situ instrumentation and there are few available microwave ground based remote sensing data sets, e. g.[1], [2], [3]. This presentation focuses on the separation of breaking and not breaking waves and the estimation of the energy dissipation of the non-breaking waves of the wave field propagating the last nautical mile towards the coast under different meteorological and oceanographic conditions.

2. METHODOLOGY

The area of investigation is an exposed littoral dune coast in the German Bight. The main instrument is a ground based Dopplerized X-band radar system with horizontal polarization [4] which was mounted onshore and the antenna was directed against the direction of wave propagation to measure normalized radar cross sections and calculate Doppler velocities of the sea surface, fig. 1. In addition, meteorological, hydrographic and bathymetric data were acquired. The main characteristic of the nautical system is the coherentisation of the transmitter/ receiver module to detect the Doppler frequency shifts in 254 range cells, with spatial resolution of 7.5 m. The resulting range is 1920 m, the temporal length of the observation is 10 min with sampling frequency 1024 pulses per second; the Doppler spectra were calculated for 0.5 s. The further analysis was based on two different approaches:

At the first approach, time series, with time step 0.5 s, of radial velocity were calculated, by defining the centroid around the maximum of each Doppler spectrum. As it has be proven in previous studies e.g. [1, 5], the detection of the wave breakers and estimation of the wave breaking probability is possibly by calculating the joint histogram of NRCS and Doppler velocities, fig. 2. For the second approach, the Doppler velocity has been calculated based on the average spectrum of each radar cell of the normalized individual spectra.

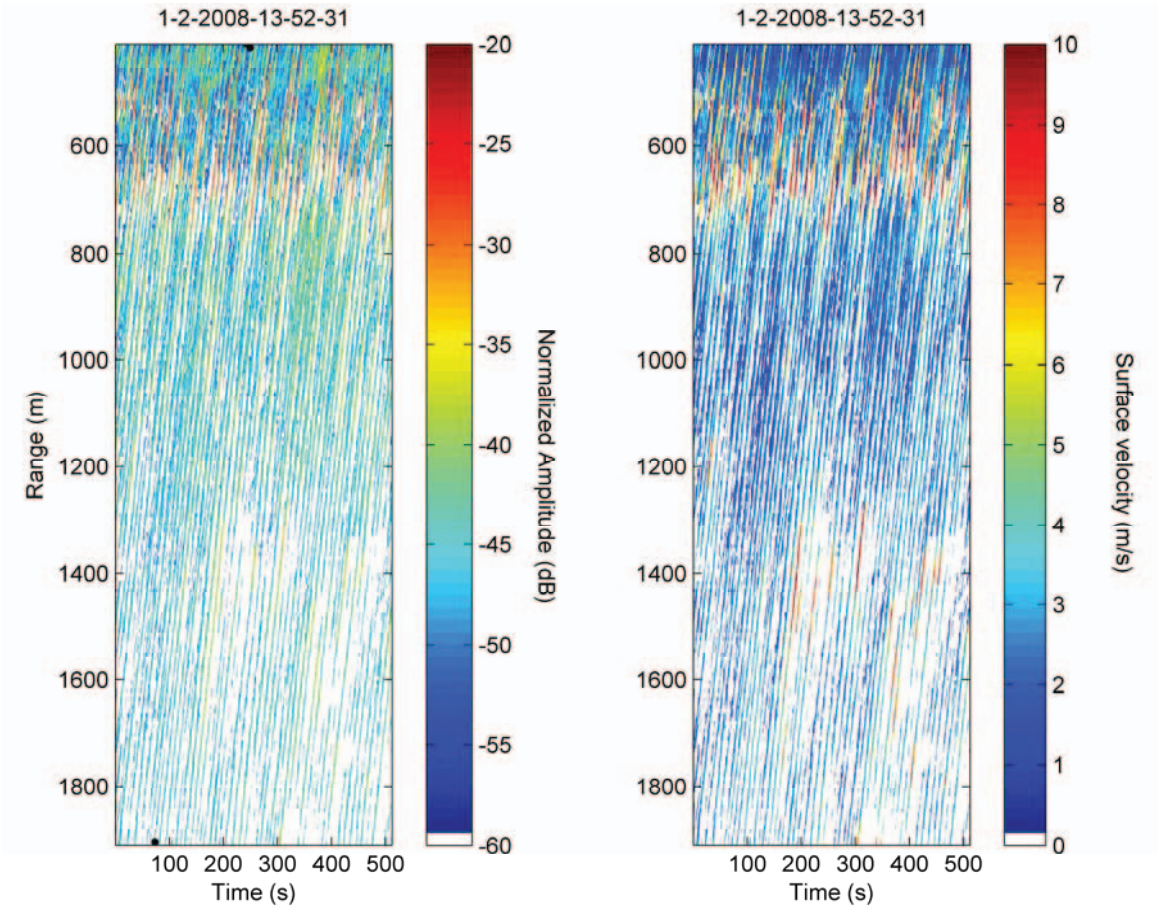

Figure 1. Range-Time-Intensity and Range-Time-Doppler velocity plots. The offshore significant wave height is 5 m during the data acquisition.

3. RESULTS AND DISCUSION

The fig. 1 shows the range-time image (RTI) of normalized radar cross, section and the associated Doppler velocity, in the direction of the wave propagation. The position $r = 0\,\mathrm{m}$ is the base of the radar mast and $t = 0\,\mathrm{s}$ is the moment of the measurement start. The NRCS values vary from -60 dB to approximately -20 dB. The permanent breaking zone starts at $r_{br_{LW}} = 750\,\mathrm{m}$, where a sand reef exists; the shoreline is at $r_{br_{BCH}} = 450\,\mathrm{m}$. At the first breaking zone, the reflectivity from the sea surface increase to values above the -35 dB and at the second above -20 dB. The large NRCS features are obvious at both breaking zones and randomly. The eliminated values (white color) correspond to the shadowed areas; the remaining values correspond to the wave crests.

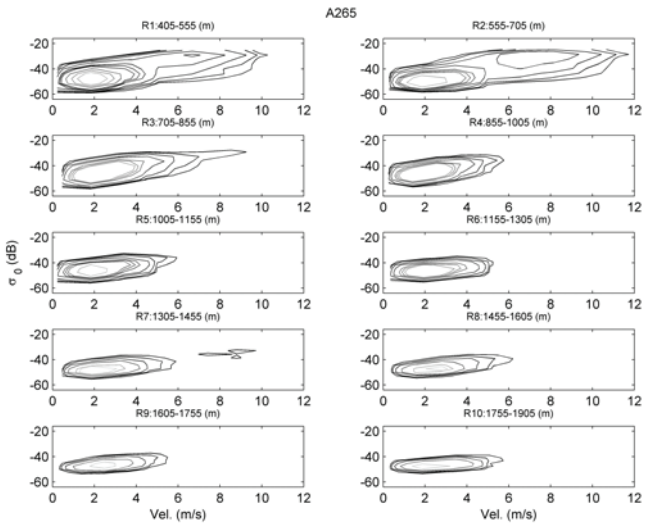

Figure 2. Contour plots of joint histograms of NRCS and Doppler velocity, for every 150 m. The bin size of the NRCS is set to 4 dB and the bin size of the Doppler velocity is set 0.4 m/s. The offshore significant wave height during the data acquisition is 5 m.

In addition, the area between the coast and the first breaking zone, it is less shadowed. This is due to the different grazing angle, for HH polarization, the geometric shadow is reasonable approximation at LGA [6]. At the breaking the highest values of the NRCS correspond also to the highest Doppler velocities.

The joint histograms of the NRCS and the Doppler velocities were calculated, fig. 2. At all the subareas, there is a main peak at the bin of -48 dB, which is corresponded to the Doppler velocity range from approximately 1.6 m/s at R1 and R2 up to 2.6 m/s at the most far regions, R8-R10. At the breaking zones, R1-R3, there is a second cluster at the bin -24 dB, the radial velocity in this clusters ranges from 6.5 m/s to 8.5 m/s, which is comparable with the phase velocity. It is proved, e.g. by [1], that the Doppler velocities of the breakers is in the same order with the wave phase velocity, which is also valid in those measurements.

To measure the mean radial velocity of the propagating waves and of breakers 2 different methods were applied; the first one by calculating directly the mean and the second, normalizing each individual Doppler spectrum by its maximum value and afterwards, calculating the mean value of all the Doppler spectra; this second method is also innovative, fig. 3. The color scale demonstrates the normalized spectrum distribution. As close to 1 is the value as more often the value appears, so the reddish values correspond to the mean dominant velocities of the sea surface during the measurement. The average Doppler spectra, most left plot, illustrate the spatial distribution of the velocity, which is dominated by the wave propagation outside the breaking zone and by the velocities of the wave breakers in the breaking zone. The resulted velocities of the second method demonstrate that the wave field propagates with reducing velocity, as it is expected, except over the breaking zone that the Doppler spectra appears 2 peaks (800 m – 600m) and the velocity of the second peak is approximately 7 m/s , central plot. The effect of the normalization before the averaging is obvious at the common plot of the two differently occurred spectra, outside of the breaking zone; the main peak is in the same velocity (2 m/s) and in the breaking zone there is a clear separation between the spectra corresponding to wave propagation and wave breaking. Based on the first peak the dissipation of the kinetic energy is estimated.

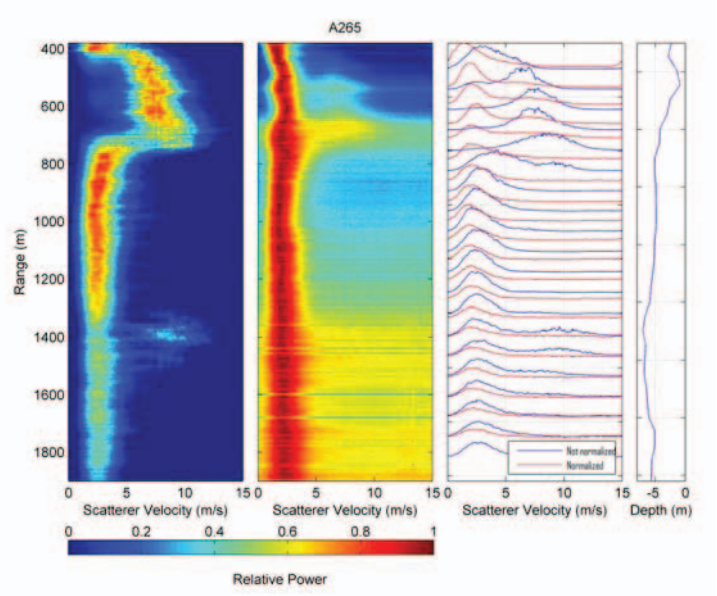

Figure 3. Left: Normalized mean Doppler velocity distribution for each radar cell and for the whole radar range, equivalent to the mean Doppler spectra. Center: Normalized mean Doppler velocity distribution of the already normalized individual Doppler spectra for each radar cell and for the whole radar range. Right: Comparison between the results of the two different processing procedures and correlation with the underlying bathymetry, H_s=5m.

4. REFERENCES

[1] G. Farquharson, S. J. Frasier, B. Raubenheimer, and S. Elgar, "Microwave radar cross sections and Doppler velocities measured in the surf zone," *J. Geophys. Res.,* vol. 110, 12/23 2005.

[2] P. Catalán, M. Haller, R. Holman, and P. W., "Surf zone breaking wave identification using marine radar," in *31st ICCE* Hamburg, 2008.

[3] S. Flampouris, F. Ziemer, and J. Seemann, "Observing littoral waves by doppler radar," in *IGARSS*, Capetown 2009.

[4] N. Braun, F. Ziemer, A. Bezuglov, M. Cysewski, and G. Schymura, "Sea-Surface Current Features Observed by Doppler Radar," *Geoscience and Remote Sensing, IEEE Transactions on,* vol. 46, pp. 1125-1133, 2008.

[5] S. Flampouris, J. Seemann, and F. Ziemer, "Observation of littoral hydrodynamics by ground based Dopplerized X-band Radar," in *Ocean Sciences Meeting*, Portland, 2010.

[6] L. B. Wetzel, "Electromagnetic scattering from the sea at low grazing angles," in *Surface waves and fluxes*. vol. 2, G. Geernaert, L. and W. Plant, L., Eds. Berlin: Springer, 1990.

[7] P. Burt, "The pyramid as structure for efficient computation," in *Multiresolution Image Processing*. vol. 12, A. Rosenfeld, Ed.: Springer, 1984, pp. 6-35.